

# Synthesis and Magnetic Properties of $\text{CuCr}_{1.65}\text{Se}_4$ Nanoparticles

E. MACIĄŻEK<sup>a</sup>, J. PANEK<sup>b</sup>, M. KUBISZTA<sup>b</sup>, M. KAROLUS<sup>b</sup>, T. GROŃC<sup>c</sup> AND H. DUDA<sup>c</sup>

<sup>a</sup>University of Silesia, Institute of Chemistry, Szkolna 9, 40-006 Katowice, Poland

<sup>b</sup>University of Silesia, Institute of Material Science, 75 Pułku Piechoty 1A, 41-500 Chorzów, Poland

<sup>c</sup>University of Silesia, Institute of Physics, Uniwersytecka 4, 40-007 Katowice, Poland

$\text{CuCr}_{1.65}\text{Se}_4$  nanoparticles crystallize in the monoclinic  $\text{Cr}_2\text{Se}_3$ -type structure of the space group  $I2/m$ . The average crystallite size basing on the line broadening is less than 10 nm. With decrease of the size of grains a change from ferromagnetic to ferrimagnetic order, a lack of the magnetization saturation and a strong spin-orbit coupling visible in the large value of the Landé factor  $g_x = 2.72$  are observed. The change in magnetic order is caused by the change of the crystalline symmetry from the cubic phase to monoclinic one.

DOI: [10.12693/APhysPolA.126.1137](https://doi.org/10.12693/APhysPolA.126.1137)

PACS: 75.50.Gg, 75.50.Tt, 81.10.Jt

## 1. Introduction

The chromium-based spinel chalcogenides,  $\text{ACr}_2\text{X}_4$  ( $\text{A} = \text{Cu}, \text{Cd}, \text{Hg}, \text{Fe}, \text{Co}$ ;  $\text{X} = \text{S}, \text{Se}, \text{Te}$ ) [1] which are ferro/ferrimagnetic insulators, semiconductors or even metals display unique properties in the bulk [2, 3]. Some of them are used as example ferrites for a radio engineering.  $\text{CuCr}_2\text{Se}_4$  is well-known as a normal spinel, ferromagnet and conductor both in the powder form as well as a single crystal [4] having the magnetization saturation of  $4.76 \mu_B/\text{f.u.}$  at 4.2 K, the effective magnetic moment of  $4.65 \mu_B/\text{f.u.}$ , the large Curie ( $T_C = 416$  K) and Curie-Weiss ( $\theta = 436$  K) temperatures [5]. The transport mechanism is here realized via a double exchange interaction involving the electrons jumping between  $\text{Cr}^{3+}$  and  $\text{Cr}^{4+}$  ions [6, 7]. This mechanism is also responsible for the thermoelectric power in  $\text{Zn}_x\text{Cu}_y\text{Cr}_z\text{Se}_4$   $p$ -type spinel conductors that the strong ferromagnetic coupling connected mainly with double-exchange and Ruderman-Kittel-Kasuya-Yosida (RKKY) mechanisms make easier the spin wave excitations [8].

Positron annihilation studies carried out on polycrystalline  $\text{CuCr}_2\text{Se}_4$  metallic conductors sintered in air and in vacuum revealed that the oxidation and adsorption processes as well as the effects of structural defects play a significant role considering the positron trapping and the corresponding linear temperature decrease of conductivity [9, 10]. The longer bulk lifetime of positrons and the lower values of the electrical conductivity observed with the  $\text{CuCr}_2\text{Se}_4$  sample sintered in air have been attributed to the scattering on the oxidation layer (surface scattering) [9, 10]. From literature it is known that in a case of manganese-zinc ferrites the conductivity of polycrystals is usually much lower than the conductivity of monocrystals of the same composition [10, 11], suggesting an influence of oxidized grain boundaries.

This paper presents the synthesis and magnetic properties of  $\text{CuCr}_{1.65}\text{Se}_4$  nanoparticles.

## 2. Experimental details

Powders of copper, chromium and selenium (99.99% purity) were mixed to give the desired composition and next they were milled in the Fritsch Pulverisette 6 planetary ball mill equipped with hardened steel vial and balls with diameter of 15 mm. The mechanical alloying process [12] was performed in a protective atmosphere of argon. The ball-to-powder weight ratio and rotational speed were 10:1 and 500 rpm, respectively. Milling times of 30 min were alternated with equal periods of rest to avoid temperature increase. After selected time intervals the samples of milled powder were examined by the X-ray diffraction method.

The XRD measurements were performed on the Philips X'Pert PW 3040/60 diffractometer using  $\text{Cu } K_\alpha$  radiation ( $\lambda = 1.54056 \text{ \AA}$ ). X'Pert HighScore Plus software and ICDD (PDF-2, 2009) files were used for phase identification. Surface morphology of compacted  $\text{CuCr}_{1.65}\text{Se}_4$  powders was studied by using a scanning microscope (JEOL JSM-6480). Magnetization and magnetic susceptibility were measured with a Quantum Design Physical Properties Measurement System (QD-PPMS) in the temperature range 1.8–360 K and at magnetic field up to 70 kOe.

## 3. Results and discussion

In Fig. 1 there are visible diffraction lines of the  $\text{Cu}_{1.96}\text{Cr}_2\text{Se}_4$  cubic phase ( $Fd-3m$ ) and traces of pure selenium and chromium after 15 h of milling. In Fig. 2 the  $\text{CuCr}_{1.65}\text{Se}_4$  monoclinic phase ( $I2/m$ ), type- $\text{Cr}_2\text{Se}_3$  with the basic lattice parameters:  $a = 6.227 \text{ \AA}$ ,  $b = 3.582 \text{ \AA}$ ,  $c = 11.528 \text{ \AA}$  and  $\beta = 90.77^\circ$  was identified in all alloys after 30, 45, 60, 85, 110 and 135 h of milling. With increase of milling time the lattice parameters are slightly decreasing and the line broadening is changing as well. In case of the diffraction lines overlapping there is possible to estimate the average crystallite size basing on

the line broadening. So, the mean crystallite sizes for as mixed powders are about: 40–60 nm after 15 h of milling, 30–40 nm after 30, 45, 60, 85 and 110 h of milling and less than 10 nm after 135 h of milling. Powders annealed at 900°C (milled 45 h and 135 h) have estimate size of crystallites in a range of 20 nm.

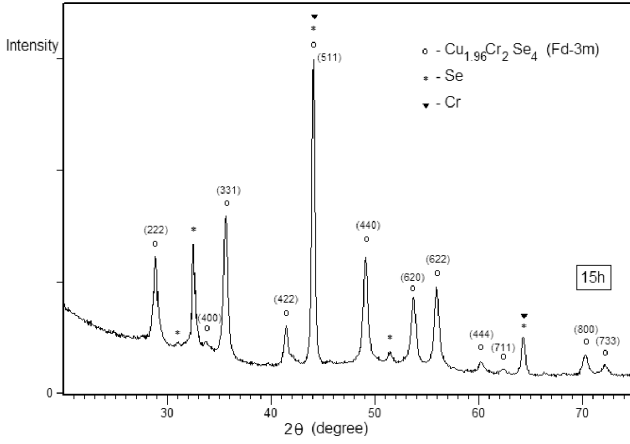


Fig. 1. XRD pattern of the  $\text{Cu}_{1.96}\text{Cr}_2\text{Se}_4$  alloy after 15 h of milling.

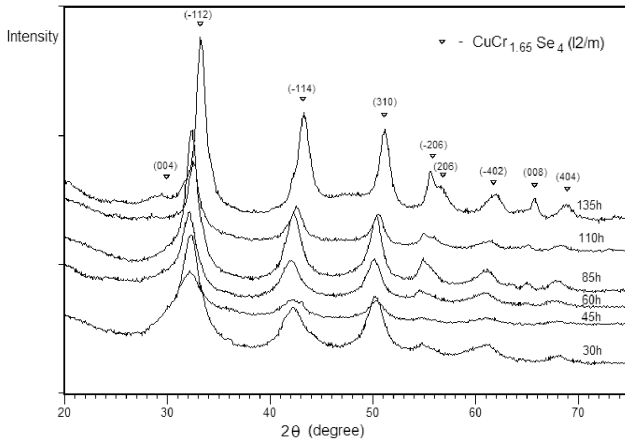


Fig. 2. XRD pattern of the  $\text{CuCr}_{1.65}\text{Se}_4$  alloys after 30, 45, 60, 85, 110, and 135 h of milling. The solid down triangles mean the peak positions for the monoclinic  $\text{Cr}_2\text{Se}_3$ -type structure for comparison.

The results of magnetic measurements presented in Figs. 3–6 and in Table showed typical behaviour for ferrimagnets. The temperature dependence of magnetic susceptibility,  $\chi(T)$ , and its reverse,  $1/\chi(T)$ , indicate a lack of the Curie–Weiss behaviour (Fig. 3). The magnetization isotherms,  $M(H)$ , show a hysteresis with coercivity of 5.6 kOe and remanence of  $0.03 \mu_B/\text{f.u.}$  at 5 K as well as a linear dependence  $M$  vs.  $H$  at 350 K (Fig. 4). The hysteresis is far from saturation because  $M = 0.23 \mu_B/\text{f.u.}$  at 70 kOe (Fig. 5). The theoretical value of the effective magnetic moment of  $\text{CuCr}_{1.65}\text{Se}_4$

is  $\mu_{\text{eff}} \approx 4.97 \mu_B/\text{f.u.}$  for a high-spin  $\text{Cr}^{3+}$  ( $S = 3/2$ ,  $g = 2$ ) is comparable with the effective number of the Bohr magnetons. This property means that the magnetic properties come mainly from the  $\text{Cr}^{3+}$  ions. The temperature dependence of the effective magnetic moment estimated from equation:  $\mu_{\text{eff}} = 2.83\sqrt{\chi T}$  strongly depends on temperature. It shows both a broad maximum around the temperature of 170 K and a broad minimum close to room temperature. At the maximum  $\mu_{\text{eff}}$  is close to the spin-only value. Upon lowering the temperature  $\mu_{\text{eff}}$  gradually decreases from  $4.77 \mu_B/\text{f.u.}$  at 170 K to  $1.21 \mu_B/\text{f.u.}$  at 5 K (Fig. 6). This behaviour is also visible in the product of  $\chi T$  in Fig. 6. It can mean that the ferrimagnetic order dominates from one side and the strong magnetocrystalline anisotropy exists in the sample from the other. Also a strong spin-orbit coupling visible in the large value of the Landé factor  $g_\chi = 2.72$  may exist, too. A superparamagnetism was not stated in the  $\text{CuCr}_{1.65}\text{Se}_4$  nanoparticles since the magnetization curves were deviated from the universal function of magnetization vs. magnetic field divided by the temperature [13].

TABLE I

Magnetic parameters of  $\text{CuCr}_{1.65}\text{Se}_4$  nanoparticles:  $C$  is the Curie constant,  $\theta$  is the Curie–Weiss temperature,  $T_C$  is the Curie temperature,  $\mu_{\text{eff}}$  is the effective magnetic moment,  $p_{\text{eff}}$  the effective number of Bohr magnetons and  $g_\chi$  is the Landé factor estimated from the Curie constant.

$C$ [emu K/mol]	$\theta$ [K]	$T_C$ [K]	$\mu_{\text{eff}}$ [ $\mu_B/\text{f.u.}$ ]	$p_{\text{eff}}$	$g_\chi$
3.461	-225	173	5.265	4.975	2.72

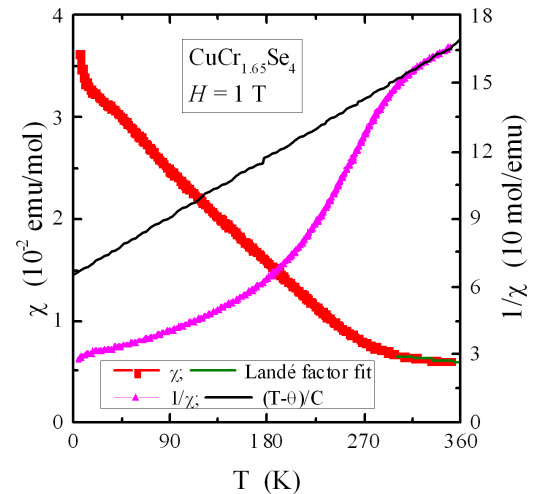


Fig. 3. Magnetic susceptibility  $\chi$  vs. temperature  $T$ . The solid (olive) line,  $C/(T - \theta)$ , is for an estimation of the Landé factor from the Curie constant. The solid (black) line,  $(T - \theta)/C$ , indicates a Curie–Weiss behavior.

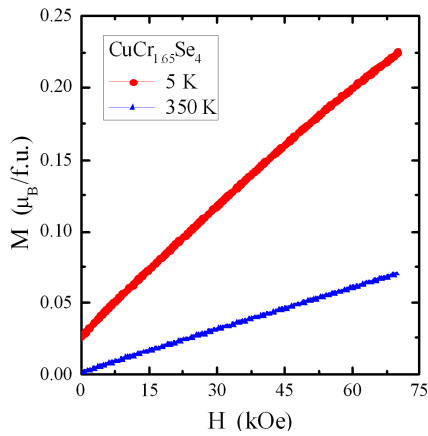


Fig. 4. Magnetization  $M$  vs. magnetic field  $H$  at 5 and 350 K.

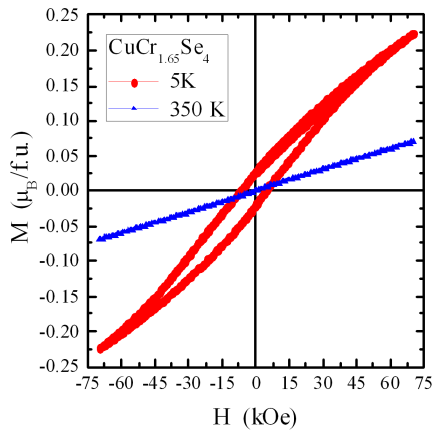


Fig. 5. Hysteresis loops at 5 and 350 K.

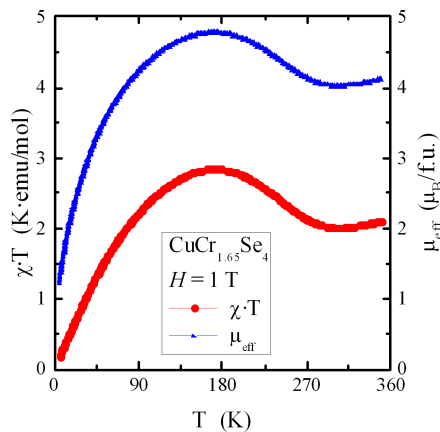


Fig. 6. Product  $\chi T$  and effective magnetic moment  $\mu_{\text{eff}}$  vs. temperature  $T$ .

## 4. Conclusions

The results of  $\text{CuCr}_{1.65}\text{Se}_4$  nanoparticles mentioned above suggest that the decrease of the size of grains causes a change both from cubic to monoclinic phase and from ferromagnetic order to ferrimagnetic one. In consequence a lack of the magnetization saturation and a strong spin-orbit coupling visible in the large value of the Landé factor  $g_{\chi} = 2.72$  are observed.

## Acknowledgments

This work was partly supported by Ministry of Scientific Research and Information Technology (Poland) and funded from science resources: No. 1S-0300-500-1-05-06. One of us (E.M.) is funded from science resources for years 2011–2014 as a research project (project No. N N204 151940).

## References

- [1] K.G. Nikiforov, *Prog. Cryst. Growth Charact. Mater.* **39**, 1 (1999).
- [2] A.P. Ramirez, R.J. Cava, J. Krajewski, *Nature* **386**, 156 (1997).
- [3] H. Brandle, J. Schoenes, P. Wachter, F. Hullinger, W. Reim, *Appl. Phys. Lett.* **56**, 2602 (1990).
- [4] *Landolt-Börnstein New Series*, Group III, Vol. 27, Part a, Ch. 1.1.5, Springer, Berlin 1988.
- [5] J. Krok, J. Spalek, S. Juszczyk, J. Warczewski, *Phys. Rev. B* **28**, 6499 (1983).
- [6] F.K. Lotgering, in: *Proc. 1964 Int. Conf. on Magnetism, Nottingham*, Ed. L.F. Bates, Institute of Physics, London 1965, p. 533.
- [7] F.K. Lotgering, R.P. Van Staple, *Solid State Commun.* **5**, 143 (1967).
- [8] T. Groń, A. Krajewski, H. Duda, P. Urbanowicz, *Physica B* **373**, 245 (2006).
- [9] T. Groń, J. Wolff, K. Bärner, I. Okońska-Kozłowska, *Solid State Phenom.* **67-68**, 335 (1999).
- [10] E. Malicka, H. Duda, T. Groń, A. Gągor, S. Mazur, J. Krok-Kowalski, *J. Phys. Chem. Solids* **73**, 262 (2012).
- [11] S. Krupička, *Physik der Ferrite und der verwandten magnetischen Oxide*, Academia Publ., Prague 1973.
- [12] C.E.M. Campos, J.C. de Lima, T.A. Grandi, K.D. Machado, P.S. Pizani, *Physica B* **324**, 409 (2002).
- [13] P. Urbanowicz, E. Tomaszewicz, T. Groń, H. Duda, A.W. Pacyna, T. Mydlarz, H. Fuks, S.M. Kaczmarek, J. Krok-Kowalski, *J. Phys. Chem. Solids* **72**, 891 (2011).